Path following strategies for non-linear analysis of steel-concrete composite sections: a bi-axial bending evaluation

Pedro H.A. Lima[1], Ígor J.M. Lemes[2], Ricardo A.M. Silveira[1], Rafael C. Barros[3]

[1] *Dept. of Civil Engineering, Federal University of Ouro Preto*
Campus Universitário s/n, Morro do Cruzeiro, 35400-000, Ouro Preto, MG, Brazil
pedro.hal@aluno.ufop.edu.br, ricardo@ufop.edu.br
[2] *Dept. of Engineering, Federal University of Lavras*
Campus Universitário, 37200-900, Lavras, MG, Brazil
igor.lemes@ufla.br
[3] *Sereng Engineering & Consulting*
34006-056, Nova Lima, Minas Gerais, Brazil
rafaelcesario@hotmail.com

Abstract. The present study aims at the non-linear analysis of steel-concrete composite cross-sections. The strain compatibility method (SCM) is used to describe the sections deformed shape in each step of the incremental-iterative solution process. For the full analysis of the moment-curvature relationship, the SCM is coupled to path-following strategies (adapted generalized displacement technique and adapted minimum residual displacement method) to go beyond the critical bending moment points in the construction of the relations that describe the complete cross-section mechanical behavior. Concomitantly, the strain-control strategy is implemented as an alternative numerical approach and used for comparison, since the bending moment limit points do not prevent the complete construction of the cross-section equilibrium path. The constitutive relationships are addressed explicitly, as well as the residual stresses present in the steel sections. To validate the proposed numerical formulation, the results obtained are compared with the numerical and experimental data available in the literature. To validate the proposed numerical formulation, the results obtained here are compared with the numerical data available in the literature. Additionally, the softening effect on the concrete was increased to induce descending stretches in the moment-curvature relationship, and this condition was correctly evaluated.

Keywords: Path-following strategies, non-linear analysis, steel-concrete composite cross-sections.

1 Introduction

The analysis of cross-sectional behavior is important to measure the parameters of its stiffness and bearing capacity, directly impacting the structural element behavior. Considering the nonlinear stress-strain relationships of materials, the numerical analysis procedures must be able to accurately capture such effects. For this evaluation, it is common to find studies that deal with the construction of interaction curves that delimit the elastic regime and the bearing capacity, for example. It is also possible to find analyzes of the cross-sectional behavior along the loading history through the moment-curvature relationship.

Bonet et al. [1] developed integration algorithms for the evaluation of reinforced concrete cross-sections subjected to biaxial bending and axial force. The decomposition of the cross-section into layers, with quadrilateral finite elements, was performed and Gauss quadrature was used to solve the integrals.Sousa Jr and Muniz [2] presented a numerical procedure for analysis of steel, reinforced concrete or composite cross-section of arbitrary polygonal shape, based on analytical evaluation of cross-section properties. The uniaxial stress–strain relationship was supposed to be of a piecewise polynomial type, and the subdivision of the section into subregions was performed by means of a contour algorithm. In a similar way, some researchers sought evaluations of the deformed state of the section for the required condition [3]. For example, Liu et al. [4] made variations in the neutral axis positions, simultaneously considering the limiting strain of some of the cross-section component materials to analyse specific interaction curves. These studies focused in generically sections shapes or determined types, as made by Li et al. [5], that analysed rectangular tubular and welded-I cross-sections using a quasi-Newton method [6].

For the evaluation of the cross-sectional behavior after the critical point of the moment-curvature relationship, Chiorean [7] presented an incremental-iterative procedure based on arc-length approach. Thus, the active bending moment was updated at each iterative cycle, making it possible to evaluate the cross-section with strains greater than those responsible for the critical bending moment. This approach was later applied in a brief study of a steel I section totally encased in concrete considering the AISC LRFD [8] and ECCS [9] residual stress models [10].

More recently, Lemes et al. [11] used the strain compatibility method (SCM) to assess the strength and also axial and bending stiffness within the context of concentrated plasticity-based formulations. The standard Newton-Raphson method was coupled to the SCM where the constitutive relationships of the materials were explicitly used. In the these researches, a simplified incremental-iterative strategy was adopted, which was interrupted when finding the moment limit point at the moment-curvature relationship. In other words, the softening parts of these relationships were not obtained. Once using constitutive relations disregarding the materials strain-softening effect, such a softening stretch is not considered.

In this sense, Caldas [12] pointed out that a simple solution to obtain the stretches with negative rigidity of the moment-curvature relationship could be found using an increment strategy based on deformations. Chiorean [13] presented a formulation for the complete construction of the moment-curvature diagrams that were determined such that axial force and bending moment ratio was kept constant. A strain-driven algorithm was developed and implemented, and the solution of the nonlinear equilibrium equations was controlled by the assumed strain values in the most compressed point and by solving just two coupled nonlinear equations.

The purpose of this work is to use path-following methods to pass through critical points in the moment-curvature relationship of cross-sections composed of steel and concrete. Utilizing the analysis of bending along the principal axes of inertia allows for predicting how a structure will behave when subjected to a load. When reaching the maximum point of the moment-curvature diagram for a normal stress value, it constitutes a failure point on the interaction surface of moments for those normal stresses. The diagrams express the behavior of the structure at each level of loading until its failure. For corrections and control in the load increment, adaptations were made in the Generalized Stiffness Parameter (GSP) [14] to the variables present in the problem addressed here. During the iterative process, the minimum residual displacement norm strategy [15] was adapted.

2 Cross-sectional analysis

The SCM is an Euler-Bernoulli Theory-based approach for the evaluation of compact cross-sections. Under external loads, a structure will gradually deform until it reaches equilibrium [8]. Once the internal and external forces are equal, the deformation stops, and, at the cross-section level, is studied by SCM [11]. In this sense, a description of the uniaxial behavior of the materials must be made for their real representation. In this work the materials are described as done in Lemes et al. [16].

2.1 Degrees of freedom

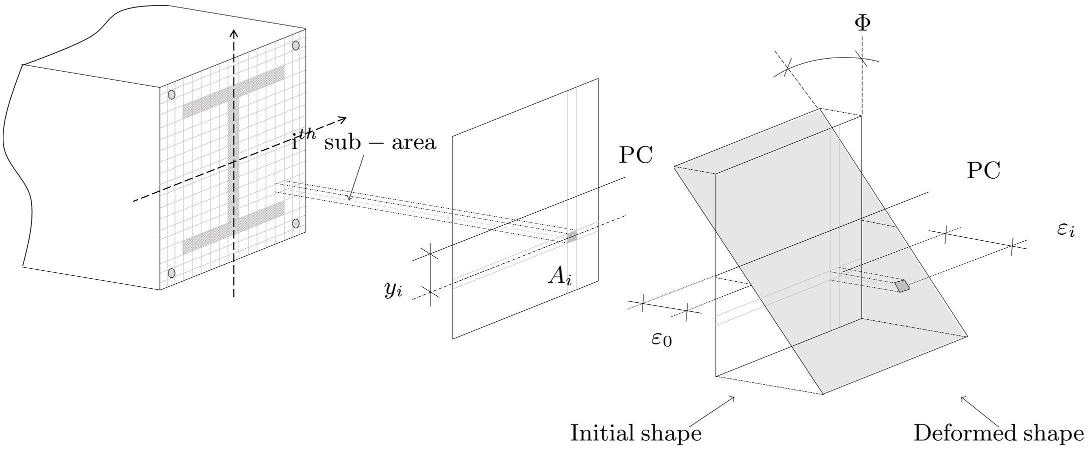

Figure 1. Linear strain field in major axis bending

The discretization shown in Figure 5 is used to find the axial strain, ε_i , in plastic centroid (PC) of each cross-sectional sub-area. Thus, through the material constitutive relationship, it is possible to obtain the respective stress, σ_i. In Figure 5, the deformed shape of an I section is illustrated for a combination of normal efforts (axial force and bending moment). Thus, the axial strain in the i^{th} sub-area can be written as follows:

$$\varepsilon_i = \varepsilon_0 + \Phi_x y_i + \Phi_y x_i + \varepsilon_{ri} \tag{1}$$

where y_i is the distance between the plastic centroids of the analyzed sub-area and the cross section, ε_0 is the axial strain of the PC section, ε_r is the strain due to residual stress, and Φ_x and Φ_y are the curvatures around the main axis. The variables ε_0 and Φ are the strain vector components.

Knowing the strain in each cross-sectional part, it is possible to determine the modulus of elasticity and the stresses acting on the materials. Thus, it is possible to assemble a system of equations that determines the cross-sectional balance, as will be discussed in the next subsections.

2.2 Constitutive matrix

The cross-section discretization shown in Figure 1 is very efficient [11] in describing the strain distribution. It is done to capture the axial strain in the center of each sub-area, and then (through the material constitutive relations) to obtain the respective stresses. Thus, the axial stress in i_{th} sub-area can be obtained by the Eq.(1).

The cross-sectional deformed shape is calculated by the equilibrium of the external, $\mathbf{f}_{ext}$, and internal, $\mathbf{f}_{int}$, forces that can be numerically expressed by the following non-linear equation:

$$\mathbf{F}(\mathbf{X}) = \underbrace{\begin{Bmatrix} N_{ext} \\ M_{ext,y} \\ M_{ext,x} \end{Bmatrix}}_{f_{ext}} - \underbrace{\begin{Bmatrix} N_{int} \cong \sum_{i=1}^{n_{fib}} \sigma\left[\varepsilon_i\left(\varepsilon_0, \Phi_y, \Phi_x\right)\right] A_i \\ M_{int,y} \cong \sum_{i=1}^{n_{fib}} \sigma\left[\varepsilon_i\left(\varepsilon_0, \Phi_y, \Phi_x\right)\right] y_i A_i \\ M_{int,x} \cong \sum_{i=1}^{n_{fib}} \sigma\left[\varepsilon_i\left(\varepsilon_0, \Phi_y, \Phi_x\right)\right] x_i A_i \end{Bmatrix}}_{f_{int}} = \begin{Bmatrix} \Delta N \\ \Delta M_y \\ \Delta M_x \end{Bmatrix} \cong \mathbf{0} \tag{2}$$

with **F** and **X** being the equilibrium force vector and strain vector, respectively, N and M are the forces, and sub-indexes int and ext are refereed to internal and external variables. All parameters are dependent of the number of degrees of freedom of the section. Applying the expansion in Taylor series in Eq.(2), results in the following set of nonlinear equations:

$$\mathbf{F(X)} = \mathbf{F'(X)}\Delta\mathbf{X} \tag{3}$$

where $\mathbf{F}'$ is the Jacobian matrix of the nonlinear problem, that is described as follow:

$$\mathbf{F}' = \left(-\frac{\partial \mathbf{F}}{\partial \mathbf{X}}\right) = \begin{bmatrix} f_{11} = \dfrac{\partial N_{int}}{\partial \varepsilon_0} & f_{12} = \dfrac{\partial N_{int}}{\partial \Phi_y} & f_{13} = \dfrac{\partial N_{int}}{\partial \Phi_x} \\ f_{21} = \dfrac{\partial M_{int,y}}{\partial \varepsilon_0} & f_{22} = \dfrac{\partial M_{int,y}}{\partial \Phi_y} & f_{23} = \dfrac{\partial M_{int,y}}{\partial \Phi_x} \\ f_{31} = \dfrac{\partial M_{int,x}}{\partial \varepsilon_0} & f_{32} = \dfrac{\partial M_{int,x}}{\partial \Phi_y} & f_{33} = \dfrac{\partial M_{int,x}}{\partial \Phi_x} \end{bmatrix} \tag{4}$$

2.3 Generalized stiffness parameters

When the cross-section equilibrium is reached, the external and internal forces vectors are numerically equal. Thus, the deformed shape of the cross-section, described by strain vector **X**, is found. For this condition, the parameters of cross-sectional stiffness are determined. In turn, the axial strains in the sub-areas are used to calculate the Jacobian matrix at this point.

Using the stiffness concept, the differentiation of force by its respective deformation defines the stiffness of the analyzed degree of freedom. As the problem has three degrees of freedom, in order to obtain the axial stiffness, the bending moments are kept constant ($\Delta M_x = 0$ and $\Delta M_y = 0$). Therefore, solving the system to determine the ratio of the force increment ΔN to the axial deformation increment $\Delta\varepsilon$ defines the axial stiffness of the section EA_T. The same process can be adapted to obtain the flexural stiffnesses $EI_{T,x}$ and $EI_{T,y}$. The calculated stiffnesses are presented as follows:

$$EI_{T,y} = \frac{\Delta M_y}{\Delta \Phi_y} = f_{33} - \left[\frac{f_{31}\left(f_{12}f_{23} - f_{13}f_{22}\right) + f_{32}\left(f_{21}f_{13} - f_{23}f_{11}\right)}{f_{11}f_{22} - f_{12}f_{21}} \right] \tag{5}$$

$$EI_{T,x} = \frac{\Delta M_x}{\Delta \Phi_x} = f_{22} - \left[\frac{f_{21}\left(f_{13}f_{32} - f_{12}f_{33}\right) + f_{23}\left(f_{12}f_{31} - f_{11}f_{32}\right)}{f_{11}f_{33} - f_{13}f_{31}} \right] \tag{6}$$

$$EA_T = \frac{\Delta N}{\Delta \varepsilon} = f_{11} - \left[\frac{f_{12}\left(f_{23}f_{31} - f_{21}f_{33}\right) + f_{13}\left(f_{32}f_{21} - f_{31}f_{22}\right)}{f_{22}f_{33} - f_{23}f_{32}} \right] \tag{7}$$

where f_{ij} are the constitutive matrix terms defined by Eq. (4)

3 Path-following strategies

In finite element context, the nonlinear static solver consists of obtaining the equilibrium between internal and external forces for each load increment as described in Eq. (2) and modified as follows [17]:

$$\mathbf{f}_{ext} - \mathbf{f}_{int} \cong 0 \rightarrow \left(\mathbf{f}_{fix} + \lambda \mathbf{f}_r\right) - \mathbf{f}_{int} \cong 0 \tag{8}$$

where $\mathbf{f}_{fix}$ is fixed forces vector, λ is the bending moment increment factor and $\mathbf{f}_r$ is the reference load vector.

To solve the nonlinear problem, load increment and iteration strategies are used.

The initial increase of the load parameter, $\Delta\lambda^0$, is automatically determined by the modified technique of generalized displacement [18]. Thus, $\Delta\lambda^0$ is calculated as:

$$\Delta\lambda^0 = \pm\Delta\lambda_1^0 \sqrt{\left| \frac{\left({}^1\delta\mathbf{X}_r^T\right)\left({}^1\delta\mathbf{X}_r\right)}{\left({}^t\delta\mathbf{X}_r^T\right)\left(\delta\mathbf{X}_r\right)} \right|} = \pm\Delta\lambda_1^0 \sqrt{|GSP|} \tag{9}$$

where index 1 indicates the $\Delta\lambda^0$ and $\delta\mathbf{X}_r$ (tangential strains) values obtained in the first loading step, and GSP represents the Generalized Stiffness Parameter.

In the traditional scheme of the Newton-Raphson method, the load parameter λ is kept constant throughout the iterative process. Thus, the equilibrium path can be obtained until a limit point and/or a bifurcation point is reached. The variation of λ during the iterative cycle enables the full equilibrium path to be traced. In this work, the minimum residual displacement norm strategy proposed by Chan [15] was used. In this strategy, the correction of the load parameter $\delta\lambda^k$ is given by the equation:

$$\delta\lambda^k = -\frac{\left(\delta\mathbf{X}_r^k\right)^T \delta\mathbf{X}_g^k}{\left(\delta\mathbf{X}_r^k\right)^T \delta\mathbf{X}_r^k} \tag{10}$$

where $\delta\mathbf{X}_g^k$ is the displacement vector correction obtained from the Newton-Raphson method application with the conventional λ increment strategy, and $\delta\mathbf{X}_r^k$ is the iterative displacement vector resulting from reference load vector $\mathbf{f}_r$ application.

4 Moment-curvature relationship

In this work, the standard Newton-Raphson method and continuation strategy were used to obtain the moment-curvature relationship. For a fixed value of axial force, N, increments are given in the external bending moment, M, until the ultimate strain of one of the materials is reached. The process of the moment-curvature relationship assessment can be seen in Figure 2:

5 Numerical application

Chiorean [10] conducted a study on the influence of residual stress models on the behavior of the steel-concrete composite section, as depicted in Figure 3. The data regarding the uniaxial behavior of materials can be seen in [10].

In Figures 4(a) - 4(c), the moment-curvature relationships obtained in this work are described for different positions of the neutral axis identified as Θ. It is possible to note that for bending about the axes of greater inertia, using the residual stress models by ECCS [9] and AISC LRFD [8], the results exhibit the same pattern. It is

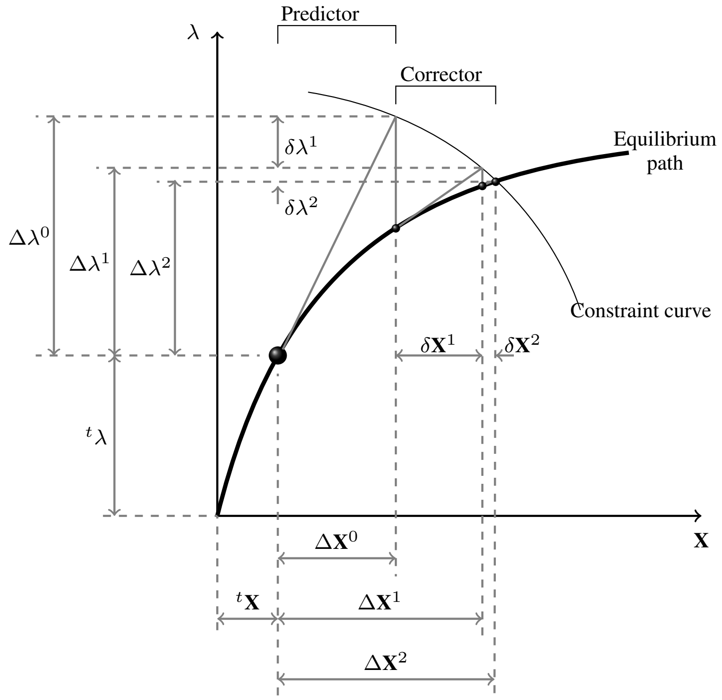

Figure 2. Numerical strategy adopted for the iterative-incremental solution

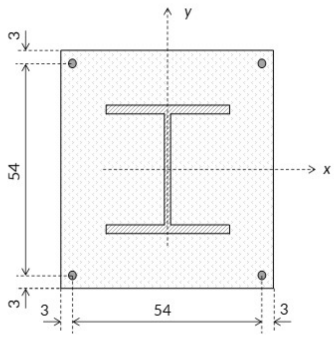

Figure 3. Rectangular composite steel-concrete cross-section

noticeable that, unlike the results presented in Lemes et al. [16], when one of the cross-sectional components of the material reaches its maximum deformation, the numerical analysis doesn't halt; instead, it captures the descending results of the moment-curvature curves.

Additionally, it can be observed that as the value of Θ increases (lowering the neutral axis), the obtained values of resisting moment decrease.

In Chiorean [19], the same cross-sectional area was also presented to assess the moment capacity contours for different axial compression load values, with and without the presence of residual stresses.

In Figure 5, it is possible to observe that the results of the present study obtained consistent outcomes with those found by Chiorean [19]. It is also noticeable the reduction in the resistant capacity of the cross-sectional area as the axial load increases, especially in the case of the EC3 distribution for residual stresses.

6 Final remarks

This work presented a numerical methodology capable of traversing the critical bending moment to evaluate the entire moment-curvature relationship.

To achieve this, the techniques of the generalized stiffness parameter [18] and minimum residual displacements [20] were coupled, both adapted to the problem of lateral deformations. In the simulated problems, it is possible to observe that the presented formulation accurately captures the behavior of the cross-sectional area when subjected to compressive loads. The choice of applying high loads is due to the occurrence of larger deformations in the section, causing it to enter the concrete softening regime.

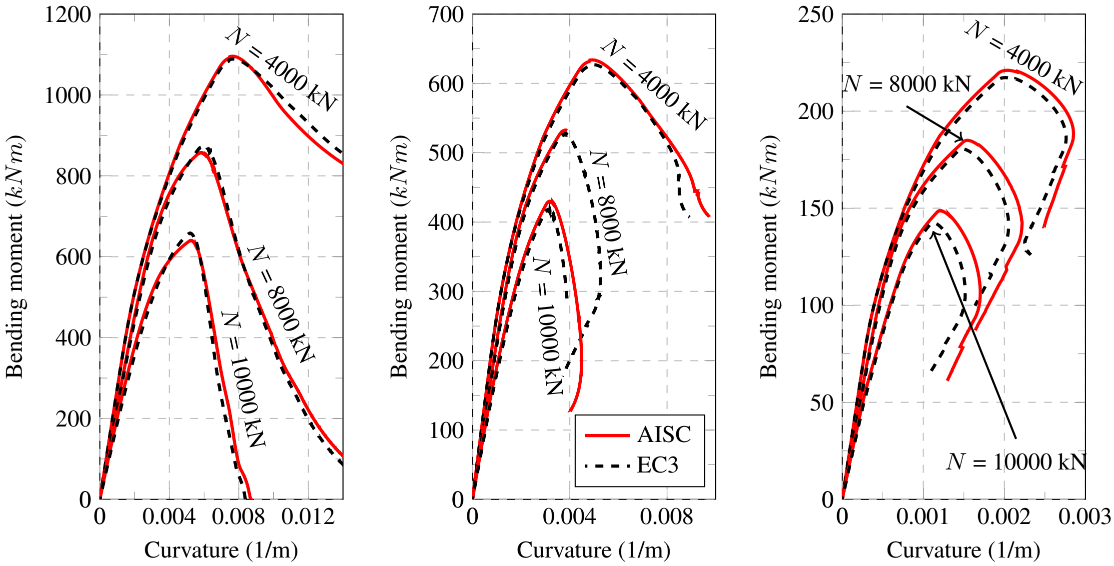

(a) $M \times \Phi$ analysis for $\theta = 15°$ (b) $M \times \Phi$ analysis for $\theta = 45°$ (c) $M \times \Phi$ analysis for $\theta = 75°$

Figure 4. Moment–curvature analysis for different values of compressive axial loads – major axis bending

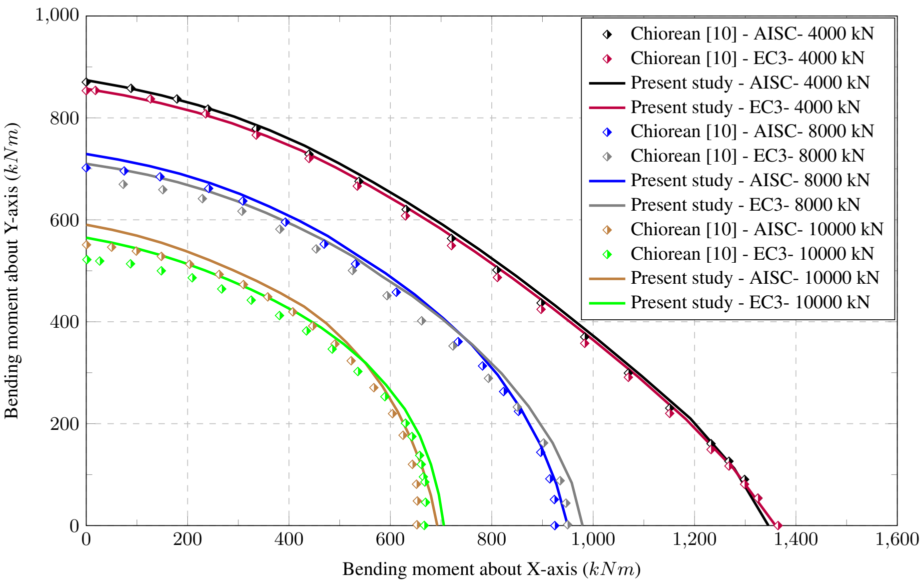

Figure 5. Moment capacity contours with different values of axial compressive load and different residual stress patterns for encased steel section

Future studies are planned regarding the extension of the proposed approach for the biaxial analysis of moment-curvature relationships in arbitrary and nonsymmetric reinforced concrete cross-sections. Based on these advanced trajectory tracking approaches, special cases associated with situations where the origins of reference axes are outside the so-called load-is contour can be accurately assessed. This allows for the precise revelation of all key features of the elastoplastic behavior of composite cross-sectional areas.

Acknowledgements. The authors would like to thank CAPES and CNPq (Federal Research Agencies), Fapemig (Minas Gerais State Research Agency), UFLA and UFOP for their support during the development of this work.

Authorship statement. The authors hereby confirm that they are the sole liable persons responsible for the authorship of this work, and that all material that has been herein included as part of the present paper is either the property (and authorship) of the authors, or has the permission of the owners to be included here.

References

[1] J. L. Bonet, M. Romero, P. Miguel, and M. Fernandez. A fast stress integration algorithm for reinforced concrete sections with axial loads and biaxial bending. *Computers Structures*, vol. 82, pp. 213–225, 2004.
[2] J. B. M. Sousa Jr and C. F. D. G. Muniz. Analytical integration of cross section properties for numerical analysis of reinforced concrete, steel and composite frames. *Engineering Structures*, vol. 29, n. 4, pp. 618–625, 2007.
[3] M. Fong and S. L. Chan. Advanced analysis of steel-concrete composite beam-columns by refined plastic-hinge method. *International Journal of Structural Stability and Dynamics*, vol. 12, n. 6, 2012.
[4] S. W. Liu, Y. P. Liu, and S. L. Chan. Advanced analysis of hybrid steel and concrete frames part 1: Cross-section analysis technique and second-order analysis. *Journal of Constructional Steel Research*, vol. 70, pp. 326–336, 2012a.
[5] T. Li, S. Liu, and S. Chan. Direct analysis for high-strength steel frames with explicit model of residual stresses. *Engineering Structures*, vol. 100, pp. 342–355, 2015.
[6] S. Chen, J. G. Teng, and S. L. Chan. Design of biaxially loaded short composite columns of arbitrary section. *Journal of Structural Engineering*, vol. 127, n. 6, pp. 678–685, 2001.
[7] C. Chiorean. Computerised interaction diagrams and moment capacity contours for composite steel–concrete cross-sections. *Engineering Structures*, vol. 32, n. 11, pp. 3734–3757, 2010.
[8] AISC LRFD. Specification for structural steel buildings. *American Institute of Steel Construction, Chicago, IL*, 2016.
[9] ECCS. Ultimate limit state calculation of sway frames with rigid joints. *European Convention for Constructional Steelwork. Technical Committee 8. Structural Stability. Technical Working Group 8.2. System*, 1984.
[10] C. G. Chiorean. A computer method for nonlinear inelastic analysis of 3D composite steel-concrete frame structures. *Engineering Structures*, vol. 57, pp. 125–152, 2013.
[11] Í. J. M. Lemes, R. A. M. Silveira, A. R. D. Silva, and P. A. S. Rocha. Nonlinear analysis of two-dimensional steel, reinforced concrete and composite steel-concrete structures via coupling SCM/RPHM. *Engineering Structures*, vol. 147, pp. 12–26, 2017.
[12] R. B. Caldas. Análise numérica de pilares mistos aço-concreto. Master's thesis, Programa de Pós Graduação em Engenharia Civil, Universidade Federal de Ouro Preto, Ouro Preto, MG, Brasil, 2004.
[13] C. Chiorean. A computer method for moment-curvature analysis of composite steel-concrete cross-sections of arbitrary shape. *Engineering Structures and Technologies*, vol. 9, n. 1, pp. 25–40, 2017.
[14] Y. Yang and S. Kuo. *Theory & analysis of nonlinear framed structures*. Prentice Hall, 1994a.
[15] S. L. Chan. Geometric and material non-linear analysis of beam-columns and frames using the minimum residual displacement method. *International Journal of Numerical Methods in Engineering*, vol. 26, n. 12, pp. 2657–2669, 1988a.
[16] Í. J. M. Lemes, P. H. A. Lima, R. C. Barros, R. A. M. Silveira, and C. G. Chiorean. A complete assessment of the moment-curvature relationship of compressed steel-concrete composite cross-sections. *ce/papers*, vol. 5, n. 3, pp. 819–827, 2022.
[17] Í. J. M. Lemes, R. C. Barros, R. A. M. Silveira, A. R. D. Silva, and P. A. S. Rocha. Numerical analysis of rc plane structures: a concentrated nonlinear effect approach. *Latin American Journal of Solids and Structures*, vol. 15, n. 2, 2018.
[18] Y.-B. Yang and S.-R. Kuo. *Theory and analysis of nonlinear framed structures*. Prentice Hall PTR, 1994b.
[19] C. Chiorean. A computer method for rapid design of composite steel-concrete crosssections. *The Open Civil Engineering Journal*, vol. 7, n. 11, pp. 1–17, 2013A.
[20] S. L. Chan. Geometric and material nonlinear analysis of beam-columns and frames using the minimum residual displacement method. *International Journal for Numerical Methods in Engineering*, vol. 26, pp. 2657–2669, 1988b.